Spontaneous *CP*-violation in the simplest little Higgs model and its future collider tests: The scalar sector

Ying-nan Mao*

Center for Future High Energy Physics and Theoretical Physics Division, Institute of High Energy Physics, Chinese Academy of Sciences, Beijing 100049, China

(Received 3 April 2017; revised manuscript received 31 October 2017; published 23 April 2018)

We propose spontaneous *CP* violation in the simplest little Higgs model. In this model, the pseudoscalar field can acquire a nonzero vacuum expectation value. This leads to a mixing between the two scalars with different *CP* charge, which means that spontaneous *CP* violation occurs. It is also a connection between the composite Higgs mechanism and *CP* violation. Facing the experimental constraints, the model is still viable for both scenarios in which the extra scalar appears below or around the electroweak scale. We also discuss the future collider tests of *CP* violation in the scalar sector through measuring h_2ZZ and h_1h_2Z' vertices (see the definitions of the particles in the text), which provide new motivations for future e^+e^- and pp colliders. This also shows the importance of the vector-vector-scalar- and vector-scalar-scalar-type vertices in discovering *CP*-violation effects in the scalar sector.

DOI: 10.1103/PhysRevD.97.075031

I. INTRODUCTION

The discovery of a 125 GeV Higgs boson [1,2] by the ATLAS and CMS collaborations [3] in 2012 implies the success of the standard model (SM) because the measured signal strengths are consistent with those predicted by the SM [4,5]. However, the electroweak symmetry-breaking (EWSB) mechanism is an important topic and research into physics beyond the SM (BSM) is still necessary and attractive.

For example, to solve the little hierarchy problem Arkani-Hamed *et al.* proposed the little Higgs (LH) framework [6] in which the collective symmetry-breaking (CSB) mechanism [6] is used to forbid the quadratic divergences in the Higgs potential at the one-loop level. The LH framework contains a lot of models. All of them are special kinds of composite Higgs models [7], and thus each of them must contain a global symmetry which is spontaneously broken at a high scale $f \gg v$, where $v = 246$ GeV is the vacuum expectation value (VEV) of the Higgs field. The SM-like Higgs boson is treated as a pseudo-Nambu-Goldstone boson corresponding to one of the broken generators, and EWSB is generated dominantly through quantum corrections; thus, the Higgs boson can be naturally light [6,7]. Usually the gauge group is also enlarged, and thus there are extra gauge bosons with masses at the $\mathcal{O}(f)$ scale. LH models are effective field theories below a cutoff scale $\Lambda \sim 4\pi f$. Below the scale Λ, a LH model is weakly coupled, but we do not know what would happen above Λ. Among these models, the simplest little Higgs (SLH) model [8–10] has a minimal extended scalar sector in which their are only two scalars. In the SLH model, a global symmetry $[\mathrm{SU}(3) \times \mathrm{U}(1)]^2$ is spontaneously broken to $[\mathrm{SU}(2) \times \mathrm{U}(1)]^2$ at the scale f. The gauge symmetry is enlarged to $\mathrm{SU}(3) \times \mathrm{U}(1)$ and spontaneously broken to the electroweak gauge symmetry $\mathrm{SU}(2)_L \times \mathrm{U}(1)$ at the scale f as well. And at the EW scale v, the gauge symmetry is further broken to $\mathrm{U}(1)_{\mathrm{em}}$, similar to the SM. If *CP* violation is absent in the scalar sector, one of the scalars is the SM-like Higgs boson (denoted as h), and the other is a pseudoscalar.

CP violation is another important topic in both SM and BSM physics. In 1964, *CP* violation was first discovered through the $K_L \to \pi\pi$ rare decay process [11]. More *CP*-violation effects have been discovered in the K- and B-meson sectors [2]. All of these measured *CP*-violation effects can be successfully explained by the Kobayashi-Maskawa (KM) mechanism [12], which was proposed by Kobayashi and Maskawa in 1973. They showed that a nontrivial *CP* phase can appear in the quark mixing matrix [called the Cabibbo-Kobayashi-Maskawa (CKM) matrix [12,13]] if there are three generations of fermions. However, the success of the KM mechanism is not the end of *CP*-violation studies. For example, the observed matter-antimatter asymmetry in the Universe [2,14] requires new sources of *CP* violation because the SM itself cannot generate such a large asymmetry [15,16]. Thus

*maoyn@ihep.ac.cn

it is attractive to study new CP-violation sources. The scalar sector is still an unfamiliar world for us and there may be lots of hidden new physics, including new sources of CP violation. Thus, in this paper we focus on extra CP violation in the scalar sector.

Theoretically, there are already many extensions of the SM that contain new CP-violation sources. For example, if we add more complex scalar singlets or doublets there may be CP violation in the scalar sector [17–21], which can lead to a CP-mixing Higgs boson.[1] Some of these models may conserve CP at the Lagrangian level and CP violation can arise only from a complex vacuum, which has been called the spontaneous CP-violation mechanism [19]. This mechanism was proposed by Lee in 1973 [19] as the first kind of two-Higgs-doublet model [17]. Moreover, the spontaneous CP-violation mechanism is also a possible solution to the strong-CP problem [23], and it may be connected with the lightness of the Higgs boson as well [24]. Besides these models, spontaneous CP violation in the scalar sector can also arise from the composite framework. There are already two examples: one is the next-to-minimal composite Higgs model [SO(6)/SO(5), or equivalently SU(4)/Sp(4)] [25], and the other is the littlest Higgs model [SU(5)/SO(5)] [26]. In these models CP violation occurs when the pseudoscalar field acquires a nonzero VEV. In this paper, we propose the possibility of spontaneous CP violation in the SLH model through the realization of the same mechanism. This model can also appear as one of the candidates to solve the strong-CP problem, as mentioned above. More details on this topic will appear in a forthcoming paper [27].

Phenomenologically, we can test new CP-violation effects directly or indirectly. Indirect effects may appear in the electric dipole moments (EDMs) of the electron and neutron [28], modifications in meson mixing parameters [29], or anomalous ZZZ couplings [30], while direct effects may be discovered in $h\tau^+\tau^-$ or $ht\bar{t}$ vertices through measuring the final-state distributions [31]. If another scalar is discovered and we denote the scalars as $h_{1,2}$ (h_1 is the SM-like Higgs boson and h_2 is the extra scalar), we can also discover CP violation in the scalar sector through directly measuring tree-level vector-vector-scalar-(VVS) and vector-scalar-scalar-type (VSS) vertices, such as h_2VV and Vh_1h_2 vertices,[2] according to the analysis of CP properties [24]. Based on this idea, we recently proposed a model-independent method to measure the CP-violation effects in the scalar sector through $e^+e^+ \to Z^* \to Zh_1$, Zh_2, h_1h_2-associated production processes at future e^+e^- colliders [32]. In that research, the product of the three vertices was used as a quantity to measure the magnitude of CP violation [32,33]. However, in the SLH model, we recently showed that the Zh_1h_2 vertex is suppressed by a factor $(v/f)^3$ [34], which means that it is difficult to test. Thus, to test CP violation in the SLH model we can turn to extra heavy gauge bosons for help.

As a summary, the model studied in this paper is attractive both theoretically and phenomenologically. This paper is organized as follows. In Sec. II we briefly review the CP-conserving SLH model, build the SLH model with spontaneous CP violation, and obtain the domain interactions. In Sec. III we consider the constraints on this model, especially in the scalar sector. In Sec. IV we discuss the tests on CP-violation effects in this model at future e^+e^- or pp colliders. In Sec. V we present our conclusions and further discussions. In the Appendix we also present the improved SLH formalism [34], which is very helpful for model building.

II. MODEL CONSTRUCTION

In this section we first briefly review the CP-conserving SLH model, and then construct the spontaneous CP-violation SLH model. We also derive the useful vertices in the spontaneous CP-violation SLH model. In both models, we have the same nonlinear realization for Goldstone bosons. We also have the same particle spectra in both models, while in the CP-violation model the scalars are both CP-mixing states. The CSB mechanism and loop corrections in the Higgs potential are also similar in both models. The difference comes from an extra explicit global $[\mathrm{SU}(3)\times\mathrm{U}(1)]^2$-breaking term which is absent in the CP-conserving model.

A. A Brief review of the CP-conserving SLH model

The SLH model contains two scalar triplets $\Phi_{1,2}$ which transform as $(\mathbf{3},\mathbf{1})$ and $(\mathbf{1},\mathbf{3})$, respectively, under the global $[\mathrm{SU}(3)\times\mathrm{U}(1)]^2$ transformation [8–10,35]. At a scale $f \gg v$, $[\mathrm{SU}(3)\times\mathrm{U}(1)]^2$ breaks to $[\mathrm{SU}(2)\times\mathrm{U}(1)]^2$ and ten Nambu-Goldstone bosons are generated, eight of which should be eaten by massive gauge bosons during spontaneous gauge symmetry breaking, $\mathrm{SU}(3)\times\mathrm{U}(1) \to \mathrm{SU}(2)_L\times\mathrm{U}(1) \to \mathrm{U}(1)_{\mathrm{em}}$. We are left with two physical scalars. The nonlinear realized scalar triples can be written as [35]

$$\Phi_1 = e^{i\Theta'}e^{it_\beta\Theta}\begin{pmatrix}\mathbf{0}_{1\times2}\\ fc_\beta\end{pmatrix}, \qquad \Phi_2 = e^{i\Theta'}e^{-i\Theta/t_\beta}\begin{pmatrix}\mathbf{0}_{1\times2}\\ fs_\beta\end{pmatrix}, \quad (1)$$

where β is a mixing angle between the two scalar triplets. The matrix fields Θ and Θ' are

[1]For the 125 GeV Higgs boson, LHC measurements prefer a CP-even one and exclude a CP-odd one above the 3σ level through the final distribution of $h \to ZZ^* \to 4\ell$ decay assuming no CP violation in the Higgs interactions [22]. However, a CP-mixing Higgs boson is still allowed since the contribution from a pseudoscalar component should be loop suppressed.

[2]Here V denotes a massive gauge boson. For the SM gauge group, $V = W$ or Z, while for LH gauge groups V can also denote extra heavy gauge bosons.

$$\Theta \equiv \frac{1}{f}\left(\frac{\eta \mathbb{I}_{3\times 3}}{\sqrt{2}} + \begin{pmatrix} \mathbf{0}_{2\times 2} & \phi \\ \phi^\dagger & 0 \end{pmatrix}\right)$$
$$\text{and} \quad \Theta' \equiv \frac{1}{f}\left(\frac{G' \mathbb{I}_{3\times 3}}{\sqrt{2}} + \begin{pmatrix} \mathbf{0}_{2\times 2} & \varphi \\ \varphi^\dagger & 0 \end{pmatrix}\right), \tag{2}$$

in which $\phi \equiv ((v_h + h - iG)/\sqrt{2}, G^-)^T$ is the usual Higgs doublet and $\varphi \equiv (y^0, x^-)^T$ is another complex doublet for Goldstones corresponding to heavy gauge bosons, following the conventions in Ref. [35].

The covariant derivative term is

$$\mathcal{L} = \sum_{i=1,2} (D^\mu \Phi_i)^\dagger (D_\mu \Phi_i), \tag{3}$$

where

$$D_\mu \equiv \partial_\mu - ig\mathbb{G}_\mu. \tag{4}$$

g is the weak coupling constant and the gauge-fields matrix is [8,9,35]

$$\mathbb{G}_\mu = \frac{A^3_\mu}{2}\begin{pmatrix} 1 & & \\ & -1 & \\ & & \end{pmatrix} + \frac{A^8_\mu}{2\sqrt{3}}\begin{pmatrix} 1 & & \\ & 1 & \\ & & -2 \end{pmatrix} + \frac{1}{\sqrt{2}}\begin{pmatrix} & W^+ & Y^0 \\ W^- & & X^- \\ \bar{Y}^0 & X^+ & \end{pmatrix}_\mu + \frac{t_W B_\mu}{3\sqrt{1 - t_W^2/3}}\mathbb{I}, \tag{5}$$

where θ_W is the EW mixing angle[3] and the complex fields $Y^0(\bar{Y}^0) \equiv (Y^1 \pm iY^2)/\sqrt{2}$. The terms including $\mathbb{G}_\mu \mathbb{G}^\mu$ in Eq. (3) give the masses of gauge bosons. Before EWSB, $v_h = 0$; after EWSB, v_h is generated through quantum corrections. It must be close to v, and their difference arises at the $\mathcal{O}((v/f)^2)$ level. To the leading order of (v/f), we have [35]

$$m_W = \frac{gv}{2} \quad \text{and} \quad m_X = m_Y = \frac{gf}{\sqrt{2}}. \tag{6}$$

The other three neutral degrees of freedom will mix with each other at leading order of (v/f) through the matrix [35]

$$\begin{pmatrix} A \\ Z \\ Z' \end{pmatrix} = \begin{pmatrix} -s_W & s_X c_W & c_X c_W \\ c_W & s_X s_W & c_X s_W \\ 0 & c_X & -s_X \end{pmatrix}\begin{pmatrix} A^3 \\ A^8 \\ B \end{pmatrix}_\mu, \tag{7}$$

where $\theta_X \equiv \arcsin(t_W/\sqrt{3})$. The corresponding masses at leading order of (v/f) are then

$$m_A = 0, \qquad m_Z = \frac{gv}{2c_W}, \quad \text{and} \quad m_{Z'} = \sqrt{\frac{2}{3 - t_W^2}}gf. \tag{8}$$

The massless gauge boson is the photon. If we go beyond the leading order of (v/f), the gauge bosons will have further mixing with each other. For example, in the charged sector $W^\pm$ and $X^\pm$ will mix with each other at the $\mathcal{O}((v/f)^3)$ level, and $W(X)^\pm$ will acquire their relative mass corrections at the $\mathcal{O}((v/f)^2)$ level. In the neutral sector, the off-diagonal elements of the mass matrix $\mathbb{M}_V^2$ in the basis (Z, Z', Y^2) are nonzero. Using an orthogonal matrix $\mathbb{R}$, it can be diagonalized as $(\mathbb{R}\mathbb{M}_V^2\mathbb{R}^T)_{pq} = m_p \delta_{pq}$, where m_p are the gauge bosons' masses. The neutral gauge bosons acquire their mass corrections as

$$\delta m_Z^2 = -\delta m_{Z'}^2 = \frac{g^2 v^2 c_{2W}^2}{32 c_W^6}\left(\frac{v}{f}\right)^2 \quad \text{and} \quad \delta m_{Y^2}^2 = 0. \tag{9}$$

We denote the corresponding mass eigenstates as $\tilde{Z}$, $\tilde{Z}'$, and $\tilde{Y}^2$. Their mixing angles (which are also approximately the rotation matrix elements) are

$$\mathbb{R}_{Z'Z} = \frac{\sqrt{3} c_{2W} c_X}{8 c_W^3}\left(\frac{v}{f}\right)^2, \qquad \mathbb{R}_{Y^2 Z} = \frac{\sqrt{2}}{3 t_{2\beta} c_W}\left(\frac{v}{f}\right)^3,$$
$$\text{and} \quad \mathbb{R}_{Y^2 Z'} = \frac{2 c_X}{\sqrt{6} t_{2\beta}}\left(\frac{v}{f}\right)^3 \tag{10}$$

to the leading order of (v/f). A and Y^1 do not participate in further mixing.

The six neutral scalar degrees of freedom can be divided into *CP*-even (h and y^1) and *CP*-odd (η, G, G', and y^2) parts, where $y^0(\bar{y}^0) \equiv (y^1 \pm iy^2)/\sqrt{2}$. A straightforward calculation shows that after EWSB the kinetic terms can be written as

$$\mathcal{L}_{\text{kin}} = \frac{1}{2}(\partial^\mu h \partial_\mu h + \partial^\mu y^1 \partial_\mu y^1 + \mathbb{K}_{ij} \partial^\mu G_i \partial_\mu G_j), \tag{11}$$

where G_i runs over the four *CP*-odd scalar degrees of freedom and $\mathbb{K}_{ij} \neq \delta_{ij}$ means the *CP*-odd part is not canonically normalized.[4] To find the canonically normalized basis, we should consider the gauge-fixing terms together. The two-point transitions between gauge bosons and scalars arise from the cross-terms of $\partial_\mu \Phi_i$ and $\mathbb{G}_\mu \Phi_i$. These transitions can be parametrized as $V_p^\mu \mathbb{F}_{pi} \partial_\mu G_i$ and their contributions should be canceled by $(\partial_\mu V_p^\mu)\mathbb{F}_{pi} G_i$ from the gauge-fixing term. It can be checked

[3] In this paper, we denote $s_\alpha \equiv \sin\alpha$, $c_\alpha \equiv \cos\alpha$, and $t_\alpha \equiv \tan\alpha$ for any angle α.

[4] Details on the improved formalism to treat this case can be found in the Appendix and Ref. [34].

straightforwardly (see the Appendix section or Ref. [34] for more details) that the new basis

$$(\tilde{\eta}, \tilde{G}_p) = \left(\frac{\eta}{\sqrt{(\mathbb{K}^{-1})_{11}}}, \frac{(\mathbb{R}\mathbb{F})_{pi}}{m_p} G_i\right) \tag{12}$$

is canonically normalized. $\tilde{G}_p$ is just the corresponding Goldstone of $\tilde{V}_p$.

In the fermion sector, each left-handed doublet must be extended to a triplet, and thus there must be additional heavy fermions. In the lepton sector, a heavy neutrino N_i should be added for each generation. Choosing the "anomaly-free embedding" [36], in the quark sector T with $Q = 2/3$ is added as the partner of t, and D and S with $Q = -1/3$ are added as the parters of d and s, respectively. The Yukawa interactions are then [8–10,35]

$$\begin{aligned}\mathcal{L}_y = {} & \mathrm{i}\lambda_N^j \bar{N}_{R,j} \Phi_2^\dagger L_j - \frac{\mathrm{i}\lambda_\ell^{jk}}{\Lambda} \bar{\ell}_{R,j} \det(\Phi_1, \Phi_2, L_k) \\ & + \mathrm{i}(\lambda_t^a \bar{u}_{R,3}^a \Phi_1^\dagger + \lambda_t^b \bar{u}_{R,3}^b \Phi_2^\dagger) Q_3 \\ & - \mathrm{i}\frac{\lambda_{b,j}}{\Lambda} \bar{d}_{R,j} \det(\Phi_1, \Phi_2, Q_3) \\ & + \mathrm{i}(\lambda_{d,n}^a \bar{d}_{R,n}^a \Phi_1^T + \lambda_{d,n}^b \bar{d}_{R,n}^b \Phi_2^T) Q_n \\ & - \mathrm{i}\frac{\lambda_u^{jk}}{\Lambda} \bar{u}_{R,j} \det(\Phi_1^*, \Phi_2^*, Q_k),\end{aligned} \tag{13}$$

where the left-handed triplets are [35]

$$\begin{aligned} & L_i = (\nu_L, \ell_L, \mathrm{i}N_L)_i^T, \qquad Q_1 = (d_L, -u_L, \mathrm{i}D_L)^T, \\ & Q_2 = (s_L, -c_L, \mathrm{i}S_L)^T, \qquad Q_3 = (t_L, b_L, \mathrm{i}T_L)^T. \end{aligned} \tag{14}$$

The first line is for leptons where $\ell_{R,j}$ runs over $(e, \mu, \tau)_R$, the second line is for the third generation of quarks where $d_{R,j}$ runs over $(d, s, b, D, S)_R$, and the last line is for the first two generations of quarks where $u_{R,j}$ runs over $(u, c, t, T)_R$. $\Lambda \sim 4\pi f$ is a cutoff scale. A right-handed quark with index a or b must be a mixing state between an additional quark and its SM partner; for example, $u_{R,3}^{a,b}$ are mixing states between t_R and T_R. To the leading order of (v/f), the heavy fermions' masses are [9,35]

$$m_N^j = \lambda_N^j f s_\beta, \qquad m_Q = \sqrt{|\lambda_q^a c_\beta|^2 + |\lambda_q^b s_\beta|^2} f, \tag{15}$$

for $Q = T$, D, S and $q = t$, $d(d_1)$, $s(d_2)$. To the leading order, the corresponding partners in the SM sector have the masses

$$m_\nu^j = 0, \qquad m_q = \frac{v}{\sqrt{2}} \frac{|\lambda_q^a \lambda_q^b|}{\sqrt{|\lambda_q^a c_\beta|^2 + |\lambda_q^b s_\beta|^2}} = \frac{\lambda_q v}{\sqrt{2}}. \tag{16}$$

The CSB mechanism keeps all neutrinos massless.[5] The other fermions acquire masses (similarly, to the leading order)

$$m_\ell^j = \frac{v}{4\sqrt{2}\pi} y_\ell^j, \qquad m_b = \frac{v}{4\sqrt{2}\pi} \lambda_{b,3}, \qquad m_{u,c} = \frac{v}{4\sqrt{2}\pi} y_{u,c}, \tag{17}$$

where y_ℓ^j are eigenvalues of matrix λ_ℓ^{jk} and $y_{u,c}$ are eigenvalues of matrix λ_u^{jk}. In this step we ignored small mixing between q and Q. If we were to consider this kind of mixing Δ_{qQ}, a mass correction $\delta m_q/m_q \sim \mathcal{O}(\Delta_{qQ}^2/m_Q^2)$ would be generated.

Last, let us turn to the scalar potential. In the discussions above, we assumed that the Higgs doublet acquires the correct VEV to derive the particle spectra everywhere. However, at tree level the $|\Phi_1^\dagger \Phi_2|^2$ term is forbidden due to the CSB mechanism. The Higgs potential can be generated through the Coleman-Weinberg mechanism [37] at loop level as

$$\delta V_h = -\delta m^2 (h^\dagger h) + \delta\lambda (h^\dagger h)^2. \tag{18}$$

The CSB mechanism forbids quadratic divergence in Eq. (18), and thus [8–10]

$$\begin{aligned}(\delta m^2)_{\text{1-loop}} = {} & \frac{3}{8\pi^2}\left(\lambda_t^2 m_T^2 \ln\frac{\Lambda^2}{m_T^2} - \frac{g^2 m_X^2}{4} \ln\frac{\Lambda^2}{m_X^2}\right. \\ & \left. - \frac{g^2 m_{Z'}^2 (1 + t_W^2)}{8} \ln\frac{\Lambda^2}{m_{Z'}^2}\right),\end{aligned} \tag{19}$$

$$\begin{aligned}(\delta\lambda)_{\text{1-loop}} = {} & \frac{(\delta m^2)_{\text{1-loop}}}{3 f^2 s_\beta^2 c_\beta^2} + \frac{3}{16\pi^2}\left(\lambda_t^4 \left(\ln\frac{m_T^2}{m_t^2} - \frac{1}{2}\right)\right. \\ & \left. - \frac{g^4}{8}\left(\ln\frac{m_X^2}{m_W^2} - \frac{1}{2}\right) - \frac{g^4 (1 + t_W^2)^2}{16}\left(\ln\frac{m_{Z'}^2}{m_Z^2} - \frac{1}{2}\right)\right).\end{aligned} \tag{20}$$

Here $\Lambda \sim 4\pi f$ is a cutoff scale and $\lambda_t \equiv \sqrt{2} m_t/v$, which means that the contributions from the first and second generations of fermions can be ignored. When m_T is heavy enough, EWSB can be generated through these loop corrections.

Now the pseudoscalar η is still massless due to an accidental global U(1) symmetry. If we add the term

$$\delta V = -\mu^2 \Phi_1^\dagger \Phi_2 + \text{H.c.} \tag{21}$$

[5] In the first term of Eq. (13) we can also use Φ_1 instead of Φ_2, but we cannot have both terms together if we assume massless neutrinos. If we perform this replacement, m_N^j in Eq. (15) should also be changed to $\lambda_N^j f c_\beta$.

to the potential,[6] η acquires its mass [10]

$$m_\eta^2 = \frac{\mu^2}{s_\beta c_\beta}\cos\left(\frac{v}{\sqrt{2}fs_\beta c_\beta}\right) \approx \frac{\mu^2}{s_\beta c_\beta} \tag{22}$$

and the Higgs potential acquires another correction [10],

$$\begin{aligned}(\delta V_h)_\mu &= -(\delta m^2)_\mu (h^\dagger h) + (\delta\lambda)_\mu (h^\dagger h)^2 \\ &= m_\eta^2 (h^\dagger h) - \frac{m_\eta^2}{12 f^2 s_\beta^2 c_\beta^2}(h^\dagger h)^2.\end{aligned} \tag{23}$$

Two-loop contributions to δm^2 can be absorbed into the possible contributions from unknown physics at the cutoff scale Λ [6,38] which can be parametrized as $(\delta m^2)_{\text{2-loop}} = -cf^2$. We can roughly estimate $|c| \sim \mathcal{O}(10^{-2})$.

B. Spontaneous *CP* violation in the SLH model

In Eq. (21) the μ term provides the η mass. In general, μ^2 can be complex, but its argument can always be absorbed into the shift of η (which is equivalent to a rotation of Φ_i). Besides this, η cannot acquire a nonzero VEV, and thus there is no *CP* violation in the scalar potential. Comparing with the *CP*-conserving case in Sec. II A, we can add another term and Eq. (21) becomes

$$\delta V = -\mu^2 \Phi_1^\dagger \Phi_2 + \epsilon(\Phi_1^\dagger \Phi_2)^2 + \text{H.c.} \tag{24}$$

Here ϵ is also required to be small [for example, $\epsilon \lesssim \mathcal{O}((v/f)^2)$], and thus the CSB mechanism is not significantly broken. In general, μ^2 and ϵ can be complex, but we can shift η to make at least one of them real. If we choose a real μ^2, when ϵ is still complex *CP* symmetry would be explicitly broken in the scalar sector. However, if both μ^2 and ϵ are real, η is also able to acquire a nonzero VEV, which means that spontaneous *CP* violation occurs. In this paper, we focus on the spontaneous *CP*-violation case.

According to Eq. (24) and denoting $\alpha \equiv v_h/(\sqrt{2}fs_\beta c_\beta)$, we have

$$\begin{aligned}V_\eta = &-\mu^2 f^2 s_\beta c_\beta c_\alpha \cos\left(\frac{\eta}{\sqrt{2}fs_\beta c_\beta}\right) \\ &+ \epsilon f^4 s_\beta^2 c_\beta^2 c_\alpha^2 \cos\left(\frac{\sqrt{2}\eta}{fs_\beta c_\beta}\right).\end{aligned} \tag{25}$$

Minimizing this potential, we find that when

$$\mu^2 < 4\epsilon f^2 |s_\beta c_\beta c_\alpha|, \tag{26}$$

$\langle\eta\rangle = 0$ becomes unstable and thus η would acquire a nonzero VEV,

$$v_\eta \equiv \langle\eta\rangle = \pm\sqrt{2}fs_\beta c_\beta \arccos\left(\frac{\mu^2}{4\epsilon f^2 s_\beta c_\beta c_\alpha}\right), \tag{27}$$

which means that spontaneous *CP* violation is possible. For simplicity, we choose "+" in the equation above from now on. We denote $\xi \equiv v_\eta/(\sqrt{2}fs_\beta c_\beta)$, and the scalar mass term is

$$\mathcal{L}_\text{m} = -\frac{1}{2}(h,\eta)\begin{pmatrix} M^2 & \epsilon f^2 s_{2\alpha} s_{2\xi} \\ \epsilon f^2 s_{2\alpha} s_{2\xi} & 4\epsilon f^2 c_\alpha^2 s_\xi^2 \end{pmatrix}\begin{pmatrix} h \\ \eta \end{pmatrix}. \tag{28}$$

Here M should be close to 125 GeV, and it includes all of the quantum-correction effects from Eqs. (19) and (20).[7] Nonzero off-diagonal elements mean that the mass eigenstates cannot be *CP* eigenstates. Defining the mass eigenstates (in which h_1 is SM-like)

$$\begin{pmatrix} h_1 \\ h_2 \end{pmatrix} \equiv \begin{pmatrix} c_\theta & -s_\theta \\ s_\theta & c_\theta \end{pmatrix}\begin{pmatrix} h \\ \eta \end{pmatrix}, \tag{29}$$

we have the mixing angle

$$\theta = \frac{1}{2}\arctan\left(\frac{2\epsilon f^2 s_{2\alpha} s_{2\xi}}{M^2 - 4\epsilon f^2 c_\alpha^2 s_\xi^2}\right) \tag{30}$$

and scalar masses

$$m_{1,2} = \sqrt{\frac{M^2 + 4\epsilon f^2 c_\alpha^2 s_\xi^2}{2} \pm \left(\frac{M^2 - 4\epsilon f^2 c_\alpha^2 s_\xi^2}{2} c_{2\theta} + \epsilon f^2 s_{2\alpha} s_{2\xi} s_{2\theta}\right)}. \tag{31}$$

[6]This term breaks the CSB mechanism explicitly which means a quadratic divergence in the Higgs potential can be generated at the one-loop level. Thus, numerically μ should be very small compared with f. In the convention of this paper (which is the same as that in Ref. [35]), the degrees of freedom in Θ' cancel with each other, and thus η does not acquire additional mixing with y^2.

[7]These quantum corrections are not affected by the *CP* properties of the scalar sector, which means that Eqs. (19) and (20) derived in the *CP*-conserving model can be simply transported into the *CP*-violating case.

We can see that CP violation can only occur when both μ^2 and ϵ are nonzero, which means that in this model CP symmetry is also collectively broken.[8]

For the Yukawa couplings, we can also choose all real couplings, and thus there is no explicit CP violation. A complex CKM matrix can arise from the mixing between an SM quark and an extra quark, which is the same mechanism as that in Ref. [18].

C. Some useful interactions in this model

In the CP-violating SLH model, mixing between h and η can modify some of the vertices in the CP-conserving model. The hVV couplings can be parametrized as

$$\mathcal{L}_{hVV} = \frac{g^2 v}{2}\sum_V((\tilde{c}_{1,V}h_1 + \tilde{c}_{2,V}h_2)\tilde{V}\tilde{V}^*), \tag{32}$$

where $\tilde{V}$ denotes the mass eigenstates. For real vector fields, $\tilde{V}^* = \tilde{V}$. To the leading order of (v/f), we have

$$\begin{aligned} \tilde{c}_{1,W} &= c_\theta \qquad \tilde{c}_{2,W} = s_\theta, \\ \tilde{c}_{1,Z} &= -\tilde{c}_{1,Z'} = \frac{c_\theta}{2c_W^2}, \qquad \tilde{c}_{2,Z} = -\tilde{c}_{2,Z'} = \frac{s_\theta}{2c_W^2}, \end{aligned} \tag{33}$$

$$\tilde{c}_{1,X} = \frac{2c_\theta}{9t_{2\beta}^2}\left(\frac{v}{f}\right)^6, \qquad \tilde{c}_{2,X} = \frac{2s_\theta}{9t_{2\beta}^2}\left(\frac{v}{f}\right)^6, \tag{34}$$

$$\tilde{c}_{1,Y} = -\frac{2c_\theta c_{2W}}{3t_{2\beta}^2 c_W^4}\left(\frac{v}{f}\right)^6, \quad \tilde{c}_{2,Y} = -\frac{2s_\theta c_{2W}}{3t_{2\beta}^2 c_W^4}\left(\frac{v}{f}\right)^6. \tag{35}$$

Here $\tilde{c}_{i,X}$ comes from the $X^\pm$ and $W^\pm$ mixing [35], while $\tilde{c}_{i,Y}$ comes from he Z, Z', and Y^2 mixing. They arise at $\mathcal{O}((v/f)^6)$, which is extremely small compared with $\tilde{c}_{i,W/Z/Z'}$.

We parametrize the antisymmetric-type $Vh\eta$ couplings[9] as

$$\begin{aligned} \mathcal{L}_{Vh_1h_2} = &\frac{g}{2}(h_1\partial^\mu h_2 - h_2\partial^\mu h_1) \\ &\times(\tilde{c}^{as}_{Zh_1h_2}\tilde{Z}_\mu + \tilde{c}^{as}_{Z'h_1h_2}\tilde{Z}'_\mu + \tilde{c}^{as}_{Yh_1h_2}\tilde{Y}^2_\mu). \end{aligned} \tag{36}$$

The results to the leading order of (v/f) are

$$\begin{aligned} \tilde{c}^{as}_{Zh_1h_2} &= \frac{1}{2\sqrt{2}c_W^3 t_{2\beta}}\left(\frac{v}{f}\right)^3, \\ \tilde{c}^{as}_{Z'h_1h_2} &= \frac{2\sqrt{2}}{\sqrt{3-t_W^2}t_{2\beta}}\left(\frac{v}{f}\right), \qquad \tilde{c}^{as}_{Yh_1h_2} = -1, \end{aligned} \tag{37}$$

which are the same as in the CP-conserving case, since $h_1\partial^\mu h_2 - h_2\partial^\mu h_1 = h\partial^\mu\eta - \eta\partial^\mu h$.

The scalar trilinear interactions should be

$$\mathcal{L}_S = -\frac{1}{2}\lambda_{122}fh_1h_2^2 - \frac{1}{2}\lambda_{211}fh_2h_1^2, \tag{38}$$

where to the leading order of (v/f) the dimensionless coefficients are

$$\begin{aligned} \lambda_{122} = &c_\theta(1-3s_\theta^2)\frac{\sqrt{2}\epsilon s_{2\alpha}(3c_{2\xi}-1)}{s_{2\beta}} \\ &+ s_\theta(2-3s_\theta^2)\frac{\sqrt{2}\epsilon s_{2\xi}(3c_{2\alpha}-1)}{s_{2\beta}} \\ &- 6c_\theta^2 s_\theta\frac{\sqrt{2}\epsilon c_\alpha^2 s_{2\xi}}{s_{2\beta}} + 6c_\theta s_\theta^2\frac{\lambda v}{f}, \end{aligned} \tag{39}$$

$$\begin{aligned} \lambda_{211} = &c_\theta(1-3s_\theta^2)\frac{\sqrt{2}\epsilon s_{2\xi}(3c_{2\alpha}-1)}{s_{2\beta}} \\ &- s_\theta(2-3s_\theta^2)\frac{\sqrt{2}\epsilon s_{2\alpha}(3c_{2\xi}-1)}{s_{2\beta}} + 6c_\theta^2 s_\theta\frac{\lambda v}{f} \\ &+ 6c_\theta s_\theta^2\frac{\sqrt{2}\epsilon c_\alpha^2 s_{2\xi}}{s_{2\beta}}. \end{aligned} \tag{40}$$

λ in the equations is the Higgs self-coupling constant.

The Yukawa couplings for SM leptons and quarks $f = \ell, q$ can be parametrized as

$$\mathcal{L}_y = -\sum_f\frac{m_f}{v}((c_{1,f}h_1 + c_{2,f}h_2)\bar{f}_L f_R) + \text{H.c.} \tag{41}$$

For $f = u, c, b, \nu, \ell$, the pseudoscalar degree of freedom does not couple to these fermions, and thus we have

$$c_{1,f} = c_\theta \quad \text{and} \quad c_{2,f} = s_\theta, \tag{42}$$

while for $q = d$, s, t the coupling coefficients are

$$\begin{aligned} c_{1,q} &= c_\theta + \mathrm{i}\delta_q s_\theta\frac{v}{f}\frac{c_{2\beta}+c_{2\theta_R}}{\sqrt{2}s_{2\beta}} \quad \text{and} \\ c_{2,q} &= s_\theta - \mathrm{i}\delta_q c_\theta\frac{v}{f}\frac{c_{2\beta}+c_{2\theta_R}}{\sqrt{2}s_{2\beta}}. \end{aligned} \tag{43}$$

Here $\delta_q = -1$ for the third generation ($q = t$) and $\delta_q = +1$ for the first two generations ($q = d, s$). The imaginary parts

[8]The case where ϵ is absent was already discussed above. The case where μ^2 is absent allows a nonzero v_η, but $\xi = \pi/2$ and thus the off-diagonal elements in Eq. (31) are still zero. A shift of η (rotation of Φ) can remove this ξ, and thus it is trivial. A nontrivial ξ requires nontrivial μ^2 and ϵ.

[9]We do not consider the symmetric-type couplings $(h_1\partial^\mu h_2 + h_2\partial^\mu h_1)$ here because they cannot contribute anything in the processes with on-shell gauge boson(s).

are generated by the left-handed mixing between light and heavy quarks. $\theta_R = \arctan(t_\beta^{-1}\lambda_1/\lambda_2)$ at the leading order of v/f is the right-handed mixing angle. Here we do not consider the possible flavor-changing couplings. The Yukawa couplings including a heavy quark should be

$$\begin{aligned}\mathcal{L}_Y = -\sum_Q \frac{m_Q}{f}((c_{1,Q}h_1 + c_{2,Q}h_2)\bar{Q}_L Q_R \\ + \bar{q}((c_{1L,q}h_1 + c_{2L,q}h_2)P_L \\ + (c_{1R,q}h_1 + c_{2R,q}h_2)P_R)Q + \text{H.c.}),\end{aligned} \tag{44}$$

where $P_{L/R} = (1 \mp \gamma^5)/2$. The coefficients are

$$\begin{aligned}c_{1,Q} &= -c_\theta \frac{v}{2f}\left(\frac{s_{2\theta_R}}{s_{2\beta}}\right)^2 + \mathrm{i}\delta_Q s_\theta \frac{c_{2\beta}+c_{2\theta_R}}{\sqrt{2}s_{2\beta}}, \\ c_{2,Q} &= s_\theta \frac{v}{2f}\left(\frac{s_{2\theta_R}}{s_{2\beta}}\right)^2 - \mathrm{i}\delta_Q c_\theta \frac{c_{2\beta}+c_{2\theta_R}}{\sqrt{2}s_{2\beta}}.\end{aligned} \tag{45}$$

Here $\delta_Q = +1$ for the third generation ($Q = T$) and $\delta_Q = -1$ for the first two generations ($Q = D$, S), which are different from those for SM fermions. $s_{2\theta_R} \propto \delta_Q m_q/m_Q$, and thus for the first two generations we have $s_{2\theta_R} \ll 1$. The other four coefficients including both light and heavy quarks are

$$\begin{aligned}c_{1L,q} &= c_\theta \frac{v}{2f}\frac{(c_{2\beta}-c_{2\theta_R})s_{2\theta_R}}{s_{2\beta}^2} + \mathrm{i}\delta_Q s_\theta \frac{s_{2\theta_R}}{\sqrt{2}s_{2\beta}} \\ &= -\delta_Q c_\theta \frac{m_q}{\sqrt{2}m_Q}\frac{c_{2\beta}-c_{2\theta_R}}{s_{2\beta}} - \mathrm{i}s_\theta \frac{m_q f}{m_Q v},\end{aligned} \tag{46}$$

$$\begin{aligned}c_{2L,q} &= s_\theta \frac{v}{2f}\frac{(c_{2\beta}-c_{2\theta_R})s_{2\theta_R}}{s_{2\beta}^2} - \mathrm{i}\delta_Q c_\theta \frac{s_{2\theta_R}}{\sqrt{2}s_{2\beta}} \\ &= -\delta_Q s_\theta \frac{m_q}{\sqrt{2}m_Q}\frac{c_{2\beta}-c_{2\theta_R}}{s_{2\beta}} + \mathrm{i}c_\theta \frac{m_q f}{m_Q v},\end{aligned} \tag{47}$$

$$c_{1R,q} = \delta_Q c_\theta \frac{c_{2\beta}+c_{2\theta}}{\sqrt{2}s_{2\beta}} - \mathrm{i}s_\theta \frac{v}{2f}\left(\left(\frac{c_{2\beta}+c_{2\theta_R}}{s_{2\beta}}\right)^2 - 1\right), \tag{48}$$

$$c_{2R,q} = \delta_Q s_\theta \frac{c_{2\beta}+c_{2\theta}}{\sqrt{2}s_{2\beta}} + \mathrm{i}c_\theta \frac{v}{2f}\left(\left(\frac{c_{2\beta}+c_{2\theta_R}}{s_{2\beta}}\right)^2 - 1\right). \tag{49}$$

In the calculation of $c_{iR,q}$, the improved formalism affects their imaginary parts since the η component in G cannot be ignored due to the improved SLH formalism [34]. For the third generation, $m_t/m_T \sim \mathcal{O}(v/f)$, and thus $c_{iL,q}$ can reach $\mathcal{O}(1)$. But for the first two generations, $m_q/m_Q \ll v/f$ means that $c_{iL,q} \ll 1$.

III. RECENT CONSTRAINTS ON THE MODEL

As a BSM model, the SLH model always faces many direct and indirect constraints, such as collider searches for new particles predicted by the model and EW precision tests. The scalar sector contains an extra scalar h_2, whose properties are quite different from the SM-like scalar. If it is light enough ($m_2 < m_1/2$), it should also face the h_1 cascade decay constraint. As a model with a new *CP*-violation source, we should also discuss the EDM constraints [28]. In this paper, we do not discuss more details about quark flavor physics.

A. Direct and indirect constraints on f

In the SLH model, the modifications of the parameters S and T are sensitive to the new scale f. Thus, before LHC Run II the S and T parameter constraint [39–41] on f used to be the strictest one: $f \gtrsim (4\text{–}7)$ TeV at 95% C.L. when $t_\beta \sim (1\text{–}10)$ [42,43]. In the SLH model with spontaneous *CP* violation this constraint is similar because S and T are not sensitive to m_2 and $c_{2,W/Z}$ when $c_{2,W/Z} \ll 1$.

However, since LHC Run II began the lower limits on exotic particles have quickly increased, and hence the corresponding new physics scales have been pushed higher. In the SLH model, $\tilde{X}^\pm$ and $\tilde{Y}^0(\tilde{\bar{Y}}^0)$ gauge bosons couple to SM fermions with a suppression factor v/f, and thus it is difficult to produce them at the LHC. However, couplings between $\tilde{Z}'$ and SM fermions have the same order as those in the SM,[10] and thus $\tilde{Z}'$ searches at the LHC can provide a direct constraint on f. Recently, using 36.1 fb^{-1} luminosity at $\sqrt{s} = 13$ TeV, the ATLAS Collaboration set a new constraint $m_{Z'} \gtrsim 4.5$ TeV at 95% C.L. [44] for the sequential standard model (SSM) [45] in which Z' couples to SM fermions with same the strengths as in the SM.

In the SLH model with "anomaly-free embedding" the gauge couplings for fermions are fixed (which can be found in Refs. [9,35]). The signal strength is then [2,10,35,45]

$$\mu \equiv \frac{(\sigma_{Z'}\mathrm{Br}_{Z'\to\ell^+\ell^-})_{\mathrm{SLH}}}{(\sigma_{Z'}\mathrm{Br}_{Z'\to\ell^+\ell^-})_{\mathrm{SSM}}} = 0.36\frac{\kappa_{d/u}+1.14}{\kappa_{d/u}+0.78} \approx 0.49, \tag{50}$$

in which

$$\begin{aligned}\kappa_{d/u} &\equiv \frac{\int dx_1 dx_2 f_d(x_1) f_{\bar{d}}(x_2)\delta(x_1x_2 - m_{Z'}^2/s)}{\int dx_1 dx_2 f_u(x_1) f_{\bar{u}}(x_2)\delta(x_1x_2 - m_{Z'}^2/s)} \\ &\sim (0.2\text{–}0.25)\end{aligned} \tag{51}$$

for $m_{Z'} = (4\text{–}4.5)$ TeV, using the MSTW2008 PDF [46]. Comparing with the results shown in Ref. [44] and assuming $m_{T,D,S,N_i} > m_{Z'}/2$, it can be roughly estimated

[10]These couplings are the same in the *CP*-conserving and *CP*-violating models.

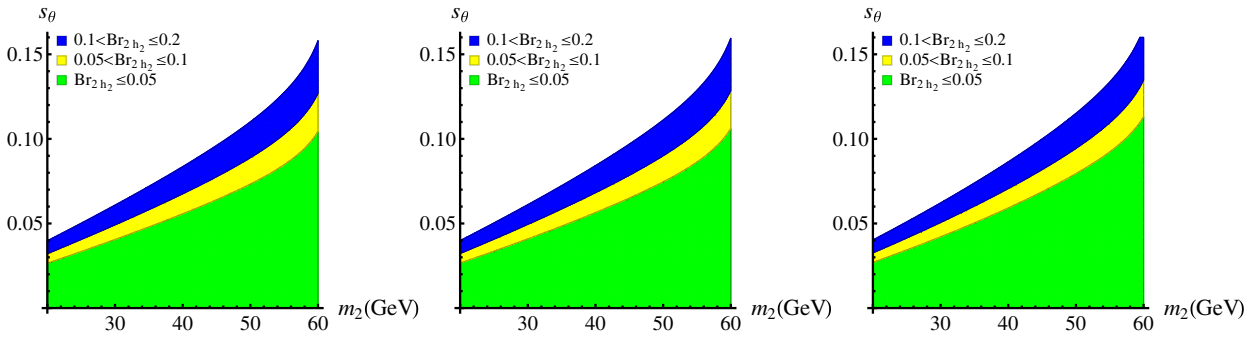

FIG. 1. The $h_1 \to 2h_2$ decay branching ratio distribution in the $s_\theta - m_2$ plane with $f = 8$ TeV. From left to right, we choose $t_\beta = 1$, 3, 6, respectively.

that $f \gtrsim 7.5$ TeV at 95% C.L.[11] Comparing with the indirect constraints discussed above, we can see that the Z' direct-search experiments can provide the strictest constraint on f in the SLH model for most of the β region.

B. Constraints on the properties of the extra scalar h_2

h_2 couples to SM particles dominantly through its h component, since the couplings between the η component and the SM sector are highly suppressed by the high scale f. Experimentally, a light h_2 could mainly be found in direct searches through $e^+e^- \to Zh_2$ at LEP, while a heavy h_2 could mainly be found in direct searches through $gg \to h_2 \to W^+W^-/ZZ$ at the LHC. Both production cross sections are suppressed by a factor s_θ^2. When $m_2 < m_1/2$, it should also face the $h_1 \to 2h_2$ rare decay constraint. Theoretically, the allowed parameter region also depends on the details of EWSB.

For $m_2 \sim (15 - 80)$ GeV, experimentally the LEP direct searches through $e^+e^- \to Z^* \to Zh_2$-associated production processes give [48]

$$s_\theta \lesssim (0.1 - 0.2) \tag{52}$$

at 95% C.L. assuming $\mathrm{Br}_{h_2 \to b\bar{b}} = 1$. $\tilde{c}_{Zh_1h_2}$ cannot be constrained at LEP since it is suppressed by a factor $(v/f)^3$. When $m_2 < m_1/2$, it must face the h_1 rare decay constraint as well. In the SLH model, the dominant exotic decay channel is $h_1 \to 2h_2$ with a branching ratio $\mathrm{Br}_{h_1 \to 2h_2} \equiv \Gamma_{h_1 \to 2h_2}/\Gamma_1$. The partial decay width is

$$\Gamma_{h_1 \to 2h_2} = \frac{\lambda_{122}^2 f^2}{32\pi m_1}\sqrt{1 - \frac{4m_2^2}{m_1^2}}, \tag{53}$$

while the h_1 total decay width is

$$\Gamma_1 = \Gamma_{h_1 \to 2h_2} + c_\theta^2 \Gamma_{1,\mathrm{SM}}. \tag{54}$$

Based on the Higgs signal strength measurements using the full 2016 data set [4,5], we perform a global fit and obtain the estimation

$$\mathrm{Br}_{\mathrm{exo}} \lesssim 0.2 \quad \text{and} \quad s_\theta \lesssim 0.4 \tag{55}$$

at 95% C.L., which is a bit stricter than the previous constraint from LHC Run I [49]. We show the branching ratio distribution in Fig. 1. According to this figure, when $m_2 \sim$ (20–60) GeV we have $s_\theta \lesssim$ (0.04–0.16), which is a stricter constraint than that from LEP direct searches. The numerical results are not sensitive to f and β.

Theoretically, the allowed parameter region also depends on the details of EWSB, especially the contributions from the cutoff scale $\delta m^2 = -cf^2$. In the CP-violation case, Eq. (23) becomes

$$\begin{aligned}\delta V_h' = {} & 2\epsilon f^2 (2c_\alpha c_{2\alpha} c_\xi^2 - c_{4\alpha} c_{2\xi})(h^\dagger h) \\ & + \frac{\epsilon(c_\alpha^2 c_\xi^2 - 2c_{2\alpha} c_{2\xi})}{3 s_\beta^2 c_\beta^2}(h^\dagger h)^2,\end{aligned} \tag{56}$$

leaving the other contributions to δV_h unchanged. For $f = 8$ TeV, in the light h_2 scenario, c is favored in the region (0.01–0.02) since a larger c_2 is excluded by the Higgs data. However, if $c \lesssim 0.01$, EWSB requires a larger s_θ which was excluded by the Higgs rare decay constraints, and thus a smaller c_2 would lead to the exclusion of a light h_2 scenario. A larger f requires a smaller c; for example, if $f = 12$ TeV, the lower limit of c reaches about 4×10^{-3}.

A heavy h_2 (with $m_2 \gtrsim 200$ GeV) is experimentally constrained by LHC direct searches. At the LHC, the gluon-fusion process acquires a dominant contribution through the top-quark loop, and the amplitudes through heavy-quark loops are suppressed by $(v/f)^2$, so $\sigma_{h_2}/\sigma_{h_2,\mathrm{SM}} \approx s_\theta^2$. If $m_2 < 2m_1$, the branching ratios of h_2 are the same as those of an SM-like Higgs boson with mass

[11]Recently, Dercks *et al.* reported a new lower limit $f \gtrsim 1.3$ TeV for the littlest Higgs model with T parity [47], which is quite lower than the limit in the SLH model. This is because in the T-parity model the extra Z' boson is T-odd, and thus it cannot have sizable couplings with SM fermion pairs. Thus, in that model direct searches for Z' cannot lead to a strict constraint on the scale f.

m_2. For $m_2 > 2m_1$, the decay channel $h_2 \to 2h_1$ opens up with a partial width

$$\Gamma_{h_2\to 2h_1} = \frac{\lambda_{211}^2 f^2}{32\pi m_2}\sqrt{1-\frac{4m_1^2}{m_2^2}}. \tag{57}$$

Its branching ratio can reach (20–30)% when $m_2 \gtrsim 300\,\mathrm{GeV}$. If $m_2 \gtrsim 350$ GeV, the $h_2 \to t\bar{t}$ decay channel can also open. Recently, the ATLAS Collaboration performed direct searches through the channels $pp \to h_2 \to W^+W-, ZZ$ for $m_2 > 200$ GeV with 36.1 fb^{-1} luminosity at $\sqrt{s} = 13$ TeV [50,51]. If $m_2 \lesssim 1$ TeV, the strictest constraints come from the $h_2 \to ZZ$ decay channel. Comparing with the SM theoretical predictions [52,53], we have the rough estimation

$$s_\theta \lesssim \begin{cases} (0.1\text{–}0.4), & \text{for } m_2 \sim (0.2\text{–}0.3)\ \text{TeV}, \\ 0.2, & \text{for } m_2 \sim (0.3\text{–}0.7)\ \text{TeV}, \\ (0.2\text{–}0.4), & \text{for } m_2 \sim (0.7\text{–}1)\ \text{TeV} \end{cases} \tag{58}$$

at 95% C.L. These constraints are a bit weaker than those in the light-m_2 region.

The theoretical constraints here are similar to those in the case with light h_2. $c \sim (0.005\text{–}0.03)$ is favored in the heavy h_2 scenario. In this scenario, the results are not sensitive to f or β. The bound on m_2 is sensitive to c but not s_θ, which is different from the properties in the light h_2 scenario.

C. EDM constraints

The EDM effective interaction can be written as

$$\mathcal{L}_{\mathrm{EDM}} = -\frac{\mathrm{i}d_f}{2}\bar{f}\sigma^{\mu\nu}\gamma^5 f F_{\mu\nu}, \tag{59}$$

which violates P and CP symmetries. In the SM, CP violation comes only from a complex CKM matrix so that the leading contributions to the EDMs of the electron and neutron arise at the four- and three-loop level, respectively. It is estimated that [28]

$$d_{e,\mathrm{SM}} \sim 10^{-38}\ e\cdot\mathrm{cm}, \qquad d_{n,\mathrm{SM}} \sim 10^{-32}\ e\cdot\mathrm{cm}, \tag{60}$$

both of which are far below the recent experimental constraints [54,55]

$$\begin{aligned} |d_e| &< 8.7\times 10^{-29}\ e\cdot\mathrm{cm}, \\ |d_n| &< 3.0\times 10^{-26}\ e\cdot\mathrm{cm} \end{aligned} \tag{61}$$

at 90% C.L. However, in some BSM models the electron or neutron EDM can be generated at the one- or two- loop level, which means that it may face strict experimental constraints.

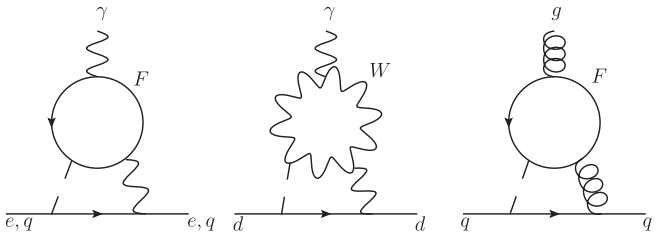

FIG. 2. Dominant Feynman diagrams contributing to the EDM of electron and quarks and the CEDM of quarks. F running in the loop includes t, T, D, S.

In the SLH model with spontaneous CP violation, the leading contribution to the electron EDM comes from the two-loop "Barr-Zee" type diagrams [56] with $F = t, T, D, S$ running in the loop (see the left diagram in Fig. 2). Following the calculations in Refs. [56,57], the analytical expression for the EDM of an electron is

$$\begin{aligned} \frac{d_e}{e} = {} & \frac{3G_F\alpha_{\mathrm{em}}m_e s_\theta c_\theta}{(2\pi)^3}\left(\frac{v}{f}\right)\sum_F Q_F^2\delta_F\frac{c_{2\beta}+c_{2\theta_{R,F}}}{s_{2\beta}} \\ & \times\left(g\left(\frac{m_F^2}{m_1^2}\right)-g\left(\frac{m_F^2}{m_2^2}\right)\right), \end{aligned} \tag{62}$$

in which the function

$$g(z) \equiv \frac{z}{2}\int_0^1 dx\frac{1}{x(1-x)-z}\ln\frac{x(1-x)}{z}. \tag{63}$$

Numerical results show that d_e is not sensitive to the masses of extra heavy quarks. For $0.2 \lesssim t_\beta \lesssim 8$, in the whole mass region $m_2 \sim (20\text{–}600)$ GeV we have

$$|d_e| \lesssim 8\times 10^{-29}\left(\frac{8\ \mathrm{TeV}}{f}\cdot\frac{s_{2\theta}}{0.2}\right)\ e\cdot\mathrm{cm} \propto f^{-1}. \tag{64}$$

The constraints from the electron EDM are not strict due to the suppressions by θ and f.

The neutron EDM comes not only from the quarks' EDM, but also their color EDM (CEDM) operator [28,56,57]

$$\mathcal{O}_{\mathrm{CEDM}} = -\frac{\mathrm{i}g_s}{2}\tilde{d}_q\bar{q}_i\sigma^{\mu\nu}\gamma^5(t^a)_{ij}q_j G^a_{\mu\nu}, \tag{65}$$

where $\tilde{d}_q$ is the CEDM of the quark, t^a denotes the color SU(3) generator, and i, j are color indices. The u-quark EDM comes only from the left diagram in Fig. 2 (just like that for the electron), while the d-quark EDM acquires contributions from both the left and middle diagrams in Fig. 2 because of the left-handed mixing between d and D quarks. The CEDMs of quarks come from the right diagram in Fig. 2. Calculated at the EW scale, the quarks' EDMs and CEDMs in the SLH model with spontaneous CP violation are [57]

$$d_u = -\frac{2m_u}{3m_e} d_e, \tag{66}$$

$$\begin{aligned} d_d = {} & \frac{m_d}{3m_e} d_e + \frac{4G_F \alpha_{\rm em} m_d s_\theta c_\theta}{9(2\pi)^3 t_\beta} \left(\frac{v}{f}\right) \left(f\left(\frac{m_t^2}{m_1^2}\right) - f\left(\frac{m_t^2}{m_2^2}\right)\right) \\ & - \frac{G_F \alpha_{\rm em} m_d s_\theta c_\theta}{12(2\pi)^3 t_\beta} \left(\frac{v}{f}\right) \\ & \times \left[\left(\left(6 + \frac{m_1^2}{m_W^2}\right) f\left(\frac{m_W^2}{m_1^2}\right) - \left(6 + \frac{m_2^2}{m_W^2}\right) f\left(\frac{m_W^2}{m_2^2}\right)\right) \right. \\ & \left. + \left(\left(10 - \frac{m_1^2}{m_W^2}\right) g\left(\frac{m_W^2}{m_1^2}\right) - \left(10 - \frac{m_2^2}{m_W^2}\right) g\left(\frac{m_W^2}{m_2^2}\right)\right)\right], \end{aligned} \tag{67}$$

$$\begin{aligned} \tilde{d}_u = {} & -\frac{G_F \alpha_s m_u s_\theta c_\theta}{2(2\pi)^3} \left(\frac{v}{f}\right) \sum_F \delta_F \frac{c_{2\beta} + c_{2\theta_{R,F}}}{s_{2\beta}} \\ & \times \left(g\left(\frac{m_F^2}{m_1^2}\right) - g\left(\frac{m_F^2}{m_2^2}\right)\right), \end{aligned} \tag{68}$$

$$\tilde{d}_d = \frac{m_d}{m_u} \tilde{d}_u - \frac{G_F \alpha_s m_d s_\theta c_\theta}{2(2\pi)^3 t_\beta} \left(\frac{v}{f}\right) \left(f\left(\frac{m_F^2}{m_1^2}\right) - f\left(\frac{m_F^2}{m_2^2}\right)\right), \tag{69}$$

in which the function

$$f(z) \equiv \frac{z}{2} \int_0^1 dx \frac{1 - 2x(1-x)}{x(1-x) - z} \ln \frac{x(1-x)}{z}. \tag{70}$$

After the running to the hadron scale, the neutron EDM is [57]

$$\frac{d_{n,\rm BZ}}{e} \simeq 0.63 \frac{d_d}{e} + 0.73 \tilde{d}_d - 0.16 \frac{d_u}{e} + 0.19 \tilde{d}_u. \tag{71}$$

Numerically, for $0.2 \lesssim t_\beta \lesssim 8$, in the whole mass region $m_2 \sim$ (20–600) GeV we have

$$|d_n| \lesssim 1.4 \times 10^{-26} \left(\frac{8\ \text{TeV}}{f} \cdot \frac{s_{2\theta}}{0.2}\right) e \cdot \text{cm}, \tag{72}$$

which is still below the experimental limit. The constraint from the neutron EDM is weaker than that from the electron EDM.

Besides the "Barr-Zee" type diagram, one-loop diagrams and the Weinberg operator [58] also contribute to the neutron EDM (see the Feynman diagrams in Fig. 3). Following Eqs. (46)–(49), we can estimate the one-loop contribution to the neutron EDM (the left and middle diagrams in Fig. 3) as

$$|\delta d_{n,\text{1-loop}}| \sim \frac{0.7 s_\theta c_\theta}{32\pi^2 t_\beta} \frac{m_d |m_1^2 - m_2^2|}{v f m_D^2} \ln\left(\frac{m_D^2}{\mu^2}\right), \tag{73}$$

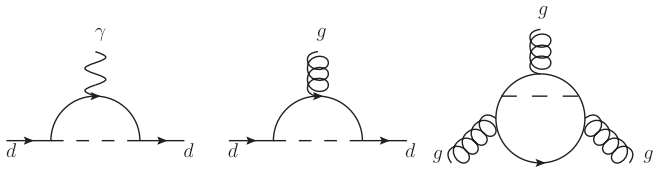

FIG. 3. Additional Feynman diagrams contributing to the neutron EDM.

where the scale $\mu \sim \mathcal{O}(v)$. This result is sensitive to m_D and m_2. For $m_D \sim \mathcal{O}(f)$ and $m_2 \lesssim \mathcal{O}(v)$, $|\delta d_{n,\text{1-loop}}| \lesssim \mathcal{O}(10^{-29}$–$10^{-27})\ e \cdot \text{cm}$. The Weinberg operator (the right diagram in Fig. 3) [58]

$$\mathcal{O}_W = -\frac{w}{3} f^{abc} G^a_{\mu\nu} G^{\nu,b}_\rho \tilde{G}^{\mu\rho,c}, \tag{74}$$

in which f^{abc} is the structure constant of the SU(3) group, contributes to the neutron EDM as [57]

$$\frac{\delta d_{n,W}}{e} \simeq (9.8\ \text{MeV}) w. \tag{75}$$

In the SLH model with spontaneous CP violation, we have

$$w = \frac{G_F \alpha_s}{(4\pi)^3} \left(\frac{v}{f}\right) s_\theta c_\theta \frac{c_{2\theta_{R,t}} + c_{2\beta}}{s_{2\beta}} \left(W\left(\frac{m_t^2}{m_2^2}\right) - W\left(\frac{m_t^2}{m_1^2}\right)\right), \tag{76}$$

where the function [57]

$$W(z) \equiv z^2 \int_0^1 du \int_0^1 dv \frac{(1-v)(uv)^3}{((1-u)(1-v) + v(1-uv)z)^2}. \tag{77}$$

Typically, $|\delta d_{n,W}| \lesssim \mathcal{O}(10^{-28})\ e \cdot \text{cm}$. Thus we can conclude that for the neutron EDM the contributions from Fig. 3 are subdominant.

There are also upper limits on heavy atoms' EDMs. The recent measurement of the ^{199}Hg atom's EDM set the new limit $|d_{\rm Hg}| < 7.4 \times 10^{-30}\ e \cdot \text{cm}$ at 95% C.L. [59], which provides an indirect constraint $d_n \lesssim 1.6 \times 10^{-26}\ e \cdot \text{cm}$ [60]. The SLH model with spontaneous CP violation is still allowed by these new indirect constraints. The theoretical estimation of the EDM of Hg contains rather large uncertainties [61], and thus it cannot directly provide further constraints on this model.

IV. FUTURE COLLIDER TESTS OF THE *CP*-VIOLATION EFFECTS

Recent Higgs data have already confirmed the 0^+ component of h_1 [22]. Following the idea in Refs. [24,32], we should try to measure the tree-level h_2VV and h_1h_2V vertices to confirm CP violation in the scalar sector. For different h_2 masses, we need different future colliders.

A. Measuring the h_2VV vertex

If h_2 is light (for example, $m_2 \ll v$), it would be difficult to discover at the LHC due to the large QCD backgrounds in the low-mass region. To test this scenario, we need future e^+e^- colliders. For example, at CEPC [62] or TLEP [63] with $\sqrt{s} \sim (240\text{–}250)$ GeV, the h_2VV vertex can be measured through the $e^+e^- \to Z^* \to Zh_2$-associated production process. Its cross section is [48,64]

$$\sigma_{Zh_2} = \frac{\pi\alpha_{\rm em}^2(8s_W^4 - 4s_W^2 + 1)\cdot s_\theta^2}{96s(1-m_Z^2/s)^2 s_W^4 c_W^4} \times \left(\mathcal{F}^3\left(\frac{m_Z^2}{s},\frac{m_2^2}{s}\right) + \frac{12m_Z^2}{s}\mathcal{F}\left(\frac{m_Z^2}{s},\frac{m_2^2}{s}\right)\right), \quad (78)$$

where the function

$$\mathcal{F}(x,y) \equiv \sqrt{1+x^2+y^2-2x-2y-2xy}. \quad (79)$$

With 5 ab^{-1} luminosity at CEPC, the inclusive discovery potential on s_θ can reach 5σ if $s_\theta \sim 0.15$ in the low-mass region ($m_2 \lesssim 70$ GeV) [32] through the "recoil mass" technique [62,65,66]. This result does not depend on the decay channel of h_2, and it is not sensitive to m_2 in this region. With the help of the "p_T balance cut" method [67] to reduce large backgrounds with photons, the 5σ discovery bound on s_θ can reach about 0.1 with a tiny breaking of inclusiveness. If we completely give up the inclusiveness in this measurement and consider only the $h_2 \to b\bar{b}$ decay channel, the 5σ discovery bound on s_θ can be suppressed to about $(4\text{–}5)\times 10^{-2}$ according to Ref. [32].[12] This result means that it is still possible to discover the allowed regions obtained in Fig. 1 at 5σ level at CEPC with 5 ab^{-1} luminosity. For larger m_2 (close to the Z peak), the large ZZ background will decrease the sensitivity on s_θ measured though this channel.

For light h_2, we can also measure s_θ through $Z \to Z^*(f\bar{f})h_2$ rare decay, if an e^+e^- collider runs at the Z pole ($\sqrt{s} = m_Z$). The branching ratio is [2]

$$\mathrm{Br}_{Z\to Z^*h_2} = \frac{s_\theta^2}{\pi^2 m_Z}\int_0^\pi \sin\phi d\phi \int_0^{m_Z-m_2} dq \frac{q^3 p_2}{(q^2-m_Z^2)^2} \times \left(2 + \frac{m_2^2\beta^2\sin^2\phi}{1-\beta^2}\right), \quad (80)$$

where q is the invariant mass of Z^*. The momentum of h_2 in the initial Z frame and the relative velocity between h_2 and Z^* are, respectively,

$$p_2 = \frac{\sqrt{(m_Z^2-(m_2-q)^2)(m_Z^2-(m_2+q)^2)}}{2m_Z}, \quad (81)$$

$$\beta = \frac{m_Z p_2}{p_2^2 + \sqrt{(p_2^2+m_2^2)(p_2^2+q^2)}}. \quad (82)$$

With 10^{12} Z-boson events as the goal of a "Tera-Z" factory, the typical sensitivity to this rare decay branching ratio is about $(10^{-8}\text{–}10^{-7})$ [68], which means that it is better suited to discovering a nonzero s_θ compared to the Zh_2-associated production channel in the whole mass region $m_2 \lesssim 70$ GeV.

For a heavy h_2 [for example, $m_2 \sim \mathcal{O}(v)$], future LHC direct searches will discover or set a stricter limit on s_θ through its ZZ decay channel [69]. Using only the visible leptonic decay channel with 3 ab^{-1}, the 5σ discovery bounds would be around $s_\theta \sim (0.1\text{–}0.2)$, which is similar to the current upper limits using the combination of $h_2 \to 4\ell$ and $h_2 \to 2\ell 2\nu$ channels [50,53,69]. We also expect that the $2\ell 2\nu$ channel can help to increase the sensitivity on s_θ at future LHC searches. When $m_2 \gtrsim 0.6$ TeV, the $2\ell 2\nu$ channel would become more sensitive than the 4ℓ channel [50].

B. Measuring the h_1h_2V vertex

Based on the improved formalism of the SLH model [34], we obtained the Zh_1h_2 vertex in Eq. (37). $\tilde{c}^{as}_{Zh_1h_2}$ is suppressed by a factor $(v/f)^3 \lesssim \mathcal{O}(10^{-5})$, and thus the associated production channels cannot be used to measure this vertex. Similarly, precision measurements on $h_1 \to Z^{(*)}h_2$ are also useless for testing this vertex, since the typical 5σ discovery bounds for such rare decay channels are of $\mathcal{O}(10^{-3})$ [62,70]. This means that we must turn to the heavy neutral gauge boson sector for help.

According to Eq. (37), $\tilde{c}^{as}_{Z'h_1h_2}$ is suppressed by a factor (v/f), and there is no suppression in $\tilde{c}^{as}_{Yh_1h_2}$. These vertices will become helpful to confirm the 0^- component in at least one of the scalars. Since $m_{Z'} \gg m_{1,2}$, the decay branching ratio is

$$\mathrm{Br}_{Z'\to h_1h_2} = \frac{m_{Z'}^3}{48\pi\Gamma_{Z'}f^2}\left(\frac{v}{ft_{2\beta}}\right)^2. \quad (83)$$

We assume that the heavy quark masses $m_F > m_{Z'}/2$, and thus $\tilde{Z}' \to F\bar{F}$ decay channels cannot be opened. The total width $\Gamma_{Z'} \approx 6.5\times 10^{-3} f$ if we choose the "anomaly-free" embedding [9]. Numerically, we have

$$\mathrm{Br}_{Z'\to h_1h_2} \simeq 1.7\times 10^{-4}\left(\frac{8\ \mathrm{TeV}}{ft_{2\beta}}\right)^2 \propto f^{-2}. \quad (84)$$

When $\beta \sim \pi/4$ this decay channel vanishes, while when β is close to 0 or $\pi/2$ there is an enhancement by $t_{2\beta}^{-2}$. It decreases quickly when f increases.

[12] Simulation details about the cross sections of the background channels were not given in the text of Ref. [32].

For this process, we need future pp colliders with larger $\sqrt{s}$ [for example, (50–100) TeV] [62,71], since at the LHC, when $m_{Z'} \gtrsim 5$ TeV, the event number of $pp \to \tilde{Z}' \to h_1 h_2$ cannot reach $\mathcal{O}(1)$ with 3 ab^{-1} luminosity [71]. However, with the same luminosity at a $\sqrt{s} = 100$ TeV pp collider, the events number can reach $N_{pp\to Z'\to h_1 h_2} \sim \mathcal{O}(10^2$–$10^3)$ for $m_{Z'} \sim 5$ TeV, and $N_{pp\to Z'\to h_1 h_2} \sim \mathcal{O}(10$–$10^2)$ for $m_{Z'} \sim 10$ TeV [71]. This implies that the $Z' h_1 h_2$ vertex in the SLH model is testable at a $\sqrt{s} = 100$ TeV pp collider.

If we can discover nonzero values for both vertices $h_2 ZZ$ and $Z' h_1 h_2$, we can confirm the CP-violation effects in the scalar sector.

V. CONCLUSIONS AND DISCUSSIONS

In this paper we proposed the possibility of spontaneous CP violation in the scalar sector of the SLH model. Through adding a new interaction term $\epsilon(\Phi_1^\dagger \Phi_2)^2 + \text{H.c.}$ in the scalar potential, the pseudoscalar field η can acquire a nonzero VEV, which means that CP violation happens spontaneously. Both scalars then become CP-mixing states. In this paper we denoted h_1 as the SM-like Higgs boson with mass $m_1 = 125$ GeV, and h_2 as the extra scalar. Based on the improved SLH formalism (see the Appendix), we derived the interactions in this model.

Facing strict experimental constraints, the spontaneous CP-violation SLH model is still not excluded. LHC Run II data have already pushed the lower limit of the scale f to about 7.5 TeV, which means that the EW precision tests only provide subdominant constraints on f. For the extra scalar h_2, we have two scenarios based on its mass: $m_2 \sim \mathcal{O}(v)$ or $m_2 \ll v$. For a light h_2, the most strict constraint comes from the $h_1 \to 2h_2$ rare decay channel. The 95% C.L. upper limit on s_θ is (0.04–0.16) for $m_2 \sim$ (20–60) GeV, while for a large $m_2 \sim \mathcal{O}(v)$ the 95% C.L. upper limit on s_θ varies in the region (0.1–0.4); in particular, when $m_2 \sim$ (300–700) GeV, the 95% C.L. upper limit on s_θ is about 0.2. In both scenarios, tiny but nonzero contributions from the cutoff scale are necessary. As a CP-violation model, it must also face the EDM constraints. Since the effects are suppressed by $s_\theta v/f$, the constraints are weak. The most strict EDM constraint comes from the electron, which favors $0.2 \lesssim t_\beta \lesssim 8$ in the whole $m_2 \sim$ (20–600) GeV mass region.

We also discussed the future collider tests of this model. The basic idea is to discover nonzero $h_2 VV$ and $V h_1 h_2$ vertices. For a light h_2, we can test the $h_2 ZZ$ vertex at future e^+e^- colliders, such as Higgs factories or a Z factory. With 5 ab^{-1} luminosity at CEPC for $m_2 \lesssim 70$ GeV, $s_\theta \sim (4$–$5) \times 10^{-2}$ can be discovered at the 5σ level, while with 10^{12} Z-boson events at the Z pole, we can have a better sensitivity in the same mass region. For a heavy h_2 with $m_2 \sim \mathcal{O}(v)$, the vertex can be tested through the $gg \to h_2 \to ZZ$ channel at the LHC. With 3 ab^{-1} luminosity, the 5σ discovery bound is around (0.1–0.2) using only the 4ℓ decay channel. The $2\ell 2\nu$ decay channel is also expected to help increase the sensitivity on s_θ, especially in the large-m_2 region. Based on the improved formalism, we know that the $Z h_1 h_2$ vertex is suppressed by $(v/f)^3$, and thus we must ask a heavy gauge boson (such as Z') for help. Since $\text{Br}_{Z'\to h_1 h_2} \lesssim \mathcal{O}(10^{-4}$–$10^{-3})$, it would be difficult to discover at the LHC. We need pp colliders with larger $\sqrt{s}$. For example, if $\sqrt{s} = 100$ TeV with 3 ab^{-1} luminosity, we can obtain $\mathcal{O}(10^2$–$10^4)$ events for the $pp \to \tilde{Z}' \to h_1 h_2$ process in the mass region $m_{Z'} \sim$ (5–10) TeV which means that it may become testable. CP violation in the scalar sector will be confirmed if nonzero $h_2 ZZ$ and $Z' h_1 h_2$ vertices are discovered.

This model is attractive both theoretically and phenomenologically. Theoretically, in this model we proposed a new possible CP-violation source, which may provide new understanding about the matter-antimatter asymmetry problem in the Universe. Besides this, the spontaneous CP-violation mechanism is also a possible solution to the strong-CP problem, which is worthy of further study. This model is also a candidate to connect the composite Higgs mechanism and CP violation in the scalar sector. Based on this, new CP-violation effects are naturally suppressed by the global symmetry-breaking scale f, as shown in the calculation of the electron and neutron EDMs.

Phenomenologically, it is an application of the basic idea of measuring $h_2 VV$ and $V h_1 h_2$ vertices. It provides an example of how extra scalars and gauge bosons can help to confirm new CP-violation sources, which also implies the importance of searching for VVS- and VSS-type vertices. It also shows another motivation for future e^+e^- and pp colliders.

ACKNOWLEDGMENTS

We thank Jordy de Vries, Shi-ping He, Fa-peng Huang, Gang Li, Jia Liu, Lian-tao Wang, Ke-pan Xie, Ling-xiao Xu, Wen Yin, Felix Yu, Chen Zhang, and Shou-hua Zhu for helpful discussions. This work was partly supported by the China Postdoctoral Science Foundation (Grant No. 2017M610992).

APPENDIX: IMPROVED FORMALISM OF THE SLH MODEL

In this appendix we present the improved formalism for the SLH model based on Ref. [34]. The neutral scalar sector (including six degrees of freedom) can be divided into CP-even and CP-odd parts. The CP-odd part—denoted as G_i and running over η, G, G', and y^2—is not canonically normalized. We can write the kinetic term as

$$\mathcal{L} \supset \frac{1}{2} \mathbb{K}_{ij} \partial^\mu G_i \partial_\mu G_j. \tag{A1}$$

The matrix elements of $\mathbb{K}$ were calculated to $\mathcal{O}((v/f)^3)$ in Ref. [34]. If we rewrite this term in another basis $S_i = U_{ij}G_j$ which is canonically normalized,

$$\mathcal{L} \supset \frac{1}{2}\delta_{ij}\partial^\mu S_i \partial_\mu S_j, \tag{A2}$$

then we can define an inner product $\langle S_i|S_j\rangle = \delta_{ij}$ in the linear space spanned by the scalars S_i. A straightforward calculation shows that

$$\langle G_i|G_j\rangle = (\mathbb{K}^{-1})_{ij}. \tag{A3}$$

The VEVs in $\Phi_{1,2}$ will lead to two-point transitions between gauge bosons and pseudoscalars as

$$\mathcal{L} \supset V_p^\mu \mathbb{F}_{pi}\partial_\mu G_i, \tag{A4}$$

where V_p denotes a gauge boson running over Z, Z', and Y^2, and $\mathbb{F}$ is a 4×3 matrix. The matrix elements of $\mathbb{F}$ were also calculated to $\mathcal{O}((v/f)^3)$ in Ref. [34]. The gauge-fixing term must provide a two-point transition like

$$\mathcal{L}_{\text{G.F.}} \supset (\partial_\mu V_p^\mu)\mathbb{F}_{pi}G_i \tag{A5}$$

to cancel all contributions from Eq. (A4). If we define

$$\bar{G}_p = \mathbb{F}_{pi}G_i \tag{A6}$$

using the convention of Ref. [35] (which is also the convention of this paper), we can derive that

$$\langle \eta|\bar{G}_p\rangle = 0, \quad \text{and} \quad \langle \bar{G}_p|\bar{G}_q\rangle = (\mathbb{M}_V^2)_{pq} \tag{A7}$$

through a straightforward calculation, where $\mathbb{M}_V^2$ is the mass matrix for gauge bosons in the basis (Z, Z', Y^2). Calculating to the leading order of (v/f) for every matrix element, we have

$$\mathbb{M}_V^2 = g^2\begin{pmatrix} \frac{v^2}{4c_W^2} & \frac{c_{2W}v^2}{4c_W^3\sqrt{3-t_W^2}} & \frac{v^3}{3\sqrt{2}c_W t_{2\beta} f} \\ \frac{c_{2W}v^2}{4c_W^3\sqrt{3-t_W^2}} & \frac{2f^2}{3-t_W^2} & \frac{v^3}{3\sqrt{6-t_W^2}c_W^2 t_{2\beta} f} \\ \frac{v^3}{3\sqrt{2}c_W t_{2\beta} f} & \frac{v^3}{3\sqrt{6-t_W^2}c_W^2 t_{2\beta} f} & \frac{f^2}{2} \end{pmatrix}. \tag{A8}$$

Using an orthogonal matrix $\mathbb{R}$, we can diagonalize $\mathbb{M}_V^2$ as

$$(\mathbb{R}\mathbb{M}_V^2\mathbb{R}^T)_{pq} = m_p^2\delta_{pq} \quad \text{and} \quad \tilde{V}_p = \mathbb{R}_{pq}V_q, \tag{A9}$$

where $\tilde{V}_p$ denotes the mass eigenstate of a gauge boson and m_p is its mass. The matrix elements of $\mathbb{R}$ were calculated to $\mathcal{O}((v/f)^3)$ in Ref. [34] as well. For simplicity, to this order the off-diagonal elements can also be expressed as

$$\mathbb{R}_{pq} = \frac{(\mathbb{M}_V^2)_{pq}}{(\mathbb{M}_V^2)_{pp} - (\mathbb{M}_V^2)_{qq}}. \tag{A10}$$

It is natural for us to define

$$\tilde{G}_p \equiv \frac{\mathbb{R}_{pq}\bar{G}_q}{m_p} = \frac{(\mathbb{R}\mathbb{F})_{pi}G_i}{m_p}. \tag{A11}$$

According to $\langle\eta|\eta\rangle = (\mathbb{K}^{-1})_{11} \approx 1 + (2/t_{2\beta}^2)(v/f)^2$, we should also define

$$\tilde{\eta} \equiv \frac{\eta}{\sqrt{(\mathbb{K}^{-1})_{11}}}. \tag{A12}$$

It is easy to check that in the basis $(\tilde{\eta}, \tilde{G}_p)$, the kinetic part is canonically normalized. Equation (A5) also becomes $m_p(\partial_\mu \tilde{V}_p^\mu)\tilde{G}_p$, and thus it is natural to choose the gauge-fixing term as

$$\mathcal{L}_{\text{G.F.}} = -\sum_p \frac{1}{2\xi_p}(\partial_\mu \tilde{V}_p^\mu - \xi_p m_p \tilde{G}_p)^2. \tag{A13}$$

It is now clear that $\tilde{G}_p$ is the corresponding Goldstone that is eaten by $\tilde{V}_p$, and its mass should be $\sqrt{\xi_p}m_p$, where ξ_p is the corresponding gauge parameter. We thus have already built the formalism to treat a model with a noncanonically normalized scalar sector, and the SLH model is one such example. The main point is that all of the two-point transitions must be carefully canceled if we do not want these kinds of Feynman diagrams appearing during the calculation.

Because of the η components in the Goldstone fields, the interactions including η must be changed compared to the naively calculated case. We divide $\mathbb{F}$ into

$$\mathbb{F} \equiv (\tilde{f}, \tilde{\mathbb{F}}), \tag{A14}$$

where $\tilde{f}_p = \mathbb{F}_{p1}$ is a 1×3 vector and $\tilde{\mathbb{F}}$ is a 3×3 matrix. Thus for any kind of couplings including the pseudoscalar degrees of freedom, if we write the coefficients as (c_η, c_j) in the G_i basis where c_j runs for the couplings including G, G' and y^2, the physical coupling should be

$$\tilde{c}_\eta = \sqrt{(\mathbb{K}^{-1})_{11}}(c_\eta - c_j(\tilde{\mathbb{F}}^{-1}\tilde{f})_j). \tag{A15}$$

For example, the antisymmetric-type $Vh\eta$ couplings in mass eigenstates can be parametrized as

$$\mathcal{L}_{Vh\eta} = \frac{g}{2}(h\partial^\mu\eta - \eta\partial^\mu h)(\tilde{c}_{Zh\eta}^{as}\tilde{Z}_\mu + \tilde{c}_{Z'h\eta}^{as}\tilde{Z}'_\mu + \tilde{c}_{Yh\eta}^{as}\tilde{Y}_\mu^2). \tag{A16}$$

With the improved formalism, we can calculate to the leading order of (v/f) as

$$\tilde{c}^{as}_{Zh\eta} = \frac{1}{2\sqrt{2}c_W^3 t_{2\beta}}\left(\frac{v}{f}\right)^3,$$
$$\tilde{c}^{as}_{Z'h\eta} = \frac{2\sqrt{2}}{\sqrt{3-t_W^2}t_{2\beta}}\left(\frac{v}{f}\right), \qquad \tilde{c}^{as}_{Yh\eta} = -1. \tag{A17}$$

The first two results are quite different from those appearing in previous papers [10,35]. Similarly, the Yukawa couplings between η and SM fermions can be parametrized as

$$\mathcal{L}_{\eta f\bar{f}} = -\sum_f c_{\eta,f}\frac{im_f}{v}\bar{f}\gamma^5 f\eta. \tag{A18}$$

According to Eq. (A15), $c_{\eta,f} = 0$ to all orders of (v/f) for $f = \nu, \ell, u, c, b$. This result is also quite different from that in previous papers [10,35]. For $f = t, d, s$, to the leading order of (v/f), we have

$$c_{\eta,f} = -\delta_f\left(\frac{v}{\sqrt{2}f}\right)\frac{c_{2\beta}+c_{2\theta}}{s_{2\beta}}, \tag{A19}$$

which is generated by the left-handed mixing between the SM fermion and additional heavy fermion. Formally, all of these results can be calculated to all orders of (v/f), though some of the results are extremely lengthy.

[1] ATLAS and CMS Collaborations, Phys. Rev. Lett. **114**, 191803 (2015).
[2] K. A. Olive *et al.* (Particle Data Group), Chin. Phys. C **38**, 090001 (2014); **40**, 100001 (2016).
[3] ATLAS Collaboration, Phys. Lett. B **716**, 1 (2012); , Phys. Lett. B **716**, 30 (2012).
[4] ATLAS Collaboration, Report No. ATLAS-CONF-2017-045; Report No. ATLAS-CONF-2017-043; Report No. ATLAS-CONF-2017-041.
[5] CMS Collaboration, Report No. CMS-PAS-HIG-16-044; Report No. CMS-PAS-HIG-16-041; Report No. CMS-PAS-HIG-16-040.
[6] N. Arkani-Hamed, A. G. Cohen, and H. Georgi, Phys. Lett. B **513**, 232 (2001); N. Arkani-Hamed, A. G. Cohen, E. Katz, and A. E. Nelson, J. High Energy Phys. 07 (2002) 034; N. Arkani-Hamed, A. G. Cohen, E. Katz, A. E. Nelson, T. Gregoire, and J. G. Wacker, J. High Energy Phys. 08 (2002) 021; M. Schmaltz and D. Tucker-Smith, Annu. Rev. Nucl. Part. Sci. **55**, 229 (2005).
[7] D. B. Kaplan and H. Georgi, Phys. Lett. B **136**, 183 (1984).
[8] D. E. Kaplan and M. Schmaltz, J. High Energy Phys. 10 (2003) 039; M. Schmaltz, J. High Energy Phys. 08 (2004) 056.
[9] T. Han, H. E. Logan, and L.-T. Wang, J. High Energy Phys. 01 (2006) 099.
[10] W. Kilian, D. Rainwater, and J. Reuter, Phys. Rev. D **71**, 015008 (2005); **74**, 095003 (2006); **74**, 099905(E) (2006); K. Cheung and J. Song, Phys. Rev. D **76**, 035007 (2007); K. Cheung, J. Song, P. Tseng, and Q.-S. Yan, Phys. Rev. D **78**, 055015 (2008).
[11] J. H. Christenson, J. W. Cronin, V. L. Fitch, and R. Turlay, Phys. Rev. Lett. **13**, 138 (1964).
[12] M. Kobayashi and T. Maskawa, Prog. Theor. Phys. **49**, 652 (1973).
[13] N. Cabibbo, Phys. Rev. Lett. **10**, 531 (1963).
[14] P. A. R. Ade *et al.* (Planck Collaboration), Astron. Astrophys. **571**, A16 (2014).
[15] D. E. Morrissey and M. J. Ramsey-Musolf, New J. Phys. **14**, 125003 (2012).
[16] A. G. Cohen, D. B. Kaplan, and A. E. Nelson, Phys. Lett. B **263**, 86 (1991); Annu. Rev. Nucl. Part. Sci. **43**, 27 (1993); J. Shu and Y. Zhang, Phys. Rev. Lett. **111**, 091801 (2013).
[17] G. C. Branco, P. M. Ferreira, L. Lavoura, M. N. Rebelo, M. Sher, and J. P. Silva, Phys. Rep. **516**, 1 (2012).
[18] L. Bento, G. C. Branco, and P. A. Parada, Phys. Lett. B **267**, 95 (1991).
[19] T. D. Lee, Phys. Rev. D **8**, 1226 (1973); Phys. Rep. **9**, 143 (1974).
[20] H. Georgi, Hadronic J. **1**, 155 (1978).
[21] S. Weinberg, Phys. Rev. Lett. **37**, 657 (1976).
[22] CMS Collaboration, Phys. Rev. D **89**, 092007 (2014); Report No. CMS-PAS-HIG-17-011; ATLAS Collaboration, Report No. ATLAS-CONF-2015-008.
[23] J. E. Kim and G. Garosi, Rev. Mod. Phys. **82**, 557 (2010); S. M. Barr, Phys. Rev. Lett. **53**, 329 (1984).
[24] Y.-N. Mao and S.-H. Zhu, Phys. Rev. D **90**, 115024 (2014); **94**, 055008 (2016); **94**, 059904(E) (2016); Y.-N. Mao, Ph.D. Thesis, Peking University, 2016.
[25] B. Gripaios, A. Pomarol, F. Riva, and J. Serra, J. High Energy Phys. 04 (2009) 070.
[26] Z. Surujon and P. Uttayarat, Phys. Rev. D **83**, 076010 (2011); H. E. Haber and Z. Surujon, Phys. Rev. D **86**, 075007 (2012).
[27] Y.-N. Mao (to be published).
[28] M. Pospelov and A. Ritz, Ann. Phys. (Amsterdam) **318**, 119 (2005).
[29] A. Hocker and Z. Ligeti, Annu. Rev. Nucl. Part. Sci. **56**, 501 (2006); J. Charles, S. Descotes-Genon, Z. Ligeti, S. Monteil, M. Papucci, and K. Trabelsi, Phys. Rev. D **89**, 033016 (2014).
[30] B. Grzadkowski, O. M. Ogreid, and P. Osland, J. High Energy Phys. 11 (2014) 084; *Proc. Sci.*, CORFU (2014) 086.
[31] S. Berge, W. Bernreuther, and J. Ziethe, Phys. Rev. Lett. **100**, 171605 (2008); S. Berge, W. Bernreuther, and S. Kirchner, Phys. Rev. D **92**, 096012 (2015); S. Berge, W. Bernreuther, and H. Spiesberger, Phys. Lett. B **727**, 488 (2013); P. S. Bhupal Dev, A. Djouadi, R. M. Godbole,

M. M. Mühlleitner, and S. D. Rindani, Phys. Rev. Lett. **100**, 051801 (2008).
[32] G. Li, Y.-N. Mao, C. Zhang, and S.-H. Zhu, Phys. Rev. D **95**, 035015 (2017).
[33] A. Méndez and A. Pomarol, Phys. Lett. B **272**, 313 (1991); J. F. Gunion and H. E. Haber, Phys. Rev. D **72**, 095002 (2005).
[34] S.-P. He, Y.-N. Mao, C. Zhang, and S.-H. Zhu, Phys. Rev. D **97**, 075005 (2018).
[35] F. del Águila, J. I. Illana, and M. D. Jenkins, J. High Energy Phys. 03 (2011) 080.
[36] O. C. W. Kong, Report No. NCU-HEP-k009, arXiv:hep-ph/0307250; J. Korean Phys. Soc. **45**, S404 (2004).
[37] S. R. Coleman and E. Weinberg, Phys. Rev. D **7**, 1888 (1973).
[38] J. A. Casas, J. R. Espinosa, and I. Hidalgo, J. High Energy Phys. 03 (2005) 038.
[39] M. E. Peskin and T. Takeuchi, Phys. Rev. Lett. **65**, 964 (1990); Phys. Rev. D **46**, 381 (1992).
[40] M. Baak, J. Cuth, J. Haller, A. Hoecker, R. Kogler, K. Mönig, M. Schott, and J. Stelzer, Eur. Phys. J. C **74**, 3046 (2014).
[41] J. de Blas, M. Ciuchini, E. Franco, S. Mishima, M. Pierini, L. Reina, and L. Silvestrini, J. High Energy Phys. 12 (2016) 135.
[42] J. Reuter and M. Tonini, J. High Energy Phys. 02 (2013) 077; M. Tonini, Report No. DESY-THESIS-2014-038; Ph.D. Thesis, Universität Hamburg, 2014.
[43] G. Marandella, C. Schappacher, and A. Strumia, Phys. Rev. D **72**, 035014 (2005).
[44] ATLAS Collaboration, J. High Energy Phys. 10 (2017) 182.
[45] P. Langacker, Rev. Mod. Phys. **81**, 1199 (2009).
[46] A. D. Martin, W. J. Stirling, R. S. Thorne, and G. Watt, Eur. Phys. J. C **63**, 189 (2009); see also http://mstwpdf.hepforge.org/.
[47] D. Dercks, G. Moortgat-Pick, J. Reuter, and S. Y. Shim, Report No. DESY-17-192, arXiv:1801.06499.
[48] ALEPH, DELPHI, L3, and OPAL Collaborations (LEP Higgs Working Group), Report No. LHWG Note/2001-04, arXiv:hep-ex/0107030; G. Abbiendi *et al.* ALEPH, DELPHI, L3, and OPAL Collaborations (LEP Higgs Working Group), Phys. Lett. B **565**, 61 (2003); S. Schael *et al.* ALEPH, DELPHI, L3, and OPAL Collaborations (LEP Higgs Working Group), Eur. Phys. J. C **47**, 547 (2006).
[49] D. Curtin *et al.*, Phys. Rev. D **90**, 075004 (2014).
[50] ATLAS Collaboration, Report No. ATLAS-CONF-2017-058.
[51] ATLAS Collaboration, Eur. Phys. J. C **78**, 24 (2018).
[52] A. Djouadi, Phys. Rep. **457**, 1 (2008); **459**, 1 (2008).
[53] LHC Higgs Cross Section Working Group, Report No. CERN-2011-002, arXiv:1101.0593; Reports No. CERN-2013-004 and No. FERMILAB-CONF-13-667-T, arXiv:1307.1347; Reports No. FERMILAB-FN-1025-T and No. CERN-2017-002-M, arXiv:1610.07922.
[54] ACME Collaboration, Science **343**, 269 (2014).
[55] C. Baker *et al.*, Phys. Rev. Lett. **97**, 131801 (2006); J. M. Pendlebury *et al.*, Phys. Rev. D **92**, 092003 (2015).
[56] S. M. Barr and A. Zee, Phys. Rev. Lett. **65**, 21 (1990); **65**, 2920(E) (1990).
[57] J. Brod, U. Haisch, and J. Zupan, J. High Energy Phys. 11 (2013) 180; T. Abe, J. Hisano, T. Kitahara, and K. Tobioka, J. High Energy Phys. 01 (2014) 106; K. Cheung, J. S. Lee, E. Senaha, and P.-Y. Tseng, J. High Energy Phys. 06 (2014) 149.
[58] S. Weinberg, Phys. Rev. Lett. **63**, 2333 (1989); D. A. Dicus, Phys. Rev. D **41**, 999 (1990); E. Braaten, C.-S. Li, and T.-C. Yuan, Phys. Rev. Lett. **64**, 1709 (1990).
[59] B. Graner, Y. Chen, E. G. Lindahl, and B. R. Heckel, Phys. Rev. Lett. **116**, 161601 (2016); **119**, 119901(E) (2017).
[60] V. F. Dmitriev and R. A. Sen'kov, Phys. Rev. Lett. **91**, 212303 (2003).
[61] J. Engel, M. J. Ramsey-Musolf, and U. van Kolck, Prog. Part. Nucl. Phys. **71**, 21 (2013); V. Cirigliano, W. Dekens, J. de Vries, and E. Mereghetti, Phys. Rev. D **94**, 034031 (2016).
[62] CEPC-SPPC Study Group, Reports No. IHEP-CEPC-DR-2015-01, No. IHEP-TH-2015-01, No. IHEP-EP-2015-01, and No. IHEP-AC-2015-01; http://cepc.ihep.ac.cn/preCDR/volume.html.
[63] M. Bicer *et al.* (TLEP Design Study Working Group), J. High Energy Phys. 01 (**2014**) 164.
[64] S. Heinemeyer and C. Schappacher, Eur. Phys J. C **76**, 220 (2016).
[65] J. F. Gunion, T. Han, and R. Sobey, Phys. Lett. B **429**, 79 (1998).
[66] NLC ZDR Design Group and NLC Physics Working Group, arXiv:hep-ex/9605011.
[67] H. Li, arXiv:1007.2999; Ph.D. Thesis, Université de Paris-Sud, 2009, http://hal.inria.fr/file/index/docid/430432/filename/Li.pdf.
[68] J. Liu, http://indico.ihep.ac.cn/event/6937/session/3/contribution/22/material/slides/0.pdf; J. Liu, L.-T. Wang, X.-P. Wang, and W. Xue, arXiv:1712.07237.
[69] CMS Collaboration, Report No. CMS-PAS-FTR-13-024.
[70] Z. Liu, L.-T. Wang, and H. Zhang, Chin. Phys. C **41**, 063102 (2017).
[71] N. Arkani-Hamed, T. Han, M. Mangano, and L.-T. Wang, Phys. Rep. **652**, 1 (2016).